



The origin of Himalayan anatexis and inverted metamorphism: Models and constraints

T. Mark Harrison*, Marty Grove, Oscar M. Lovera, E.J. Catlos, Jessica D'Andrea

Department of Earth and Space Sciences and Institute of Geophysics and Planetary Physics, University of California, Los Angeles, CA 90095-1567, USA

Abstract

The key to comprehending the tectonic evolution of the Himalaya is to understand the relationships between large-scale faulting, anatexis, and inverted metamorphism. The great number and variety of mechanisms that have been proposed to explain some or all of these features reflects the fact that fundamental constraints on such models have been slow in coming. Recent developments, most notably in geophysical imaging and geochronology, have been key to coalescing the results of varied Himalayan investigations into constraints with which to test proposed evolutionary models. These models fall into four general types: (1) the inverted metamorphic sequences within the footwall of the Himalayan thrust and adjacent hanging wall anatexis are spatially and temporally related by thrusting; (2) thrusting results from anatexis; (3) anatexis results from normal faulting; and (4) apparent inverted metamorphism in the footwall of the Himalayan thrust is produced by underplating of right-way-up metamorphic sequences. We review a number of models and find that many are inconsistent with available constraints, most notably the recognition that the exposed crustal melts and inverted metamorphic sequences not temporally related. The generalization that appears to best explain the observed distribution of crustal melts and inverted metamorphic sequences is that, due to specific petrological and tectonic controls, episodic magmatism and out-of-sequence thrusting developed during continuous convergence juxtaposing allochthonous igneous and metamorphic rocks. This coincidental juxtaposition has proven to be something of a red herring, unduly influencing attention toward finding a causal relationship between anatexis and inverted metamorphism. © 1999 Elsevier Science Ltd. All rights reserved.

1. Introduction

The extent to which we understand any evolutionary process is governed by how well we know the timing of events. Although fundamental age relationships for the most significant igneous and metamorphic activity in the Himalaya were to a large extent unknown until recently, a remarkable number and variety of contrasting tectonic models were proposed in the absence of such constraints to explain important tectonic features of the mountain belt. A common point of departure for many models seeking to account for the juxtaposition of inverted metamorphic sequences in the footwall of the Main Central Thrust (MCT) beneath higher grade rocks that host a belt of Tertiary leucogranites

(Figs. 1 and 2) was to assume that recrystallization adjacent to the MCT and anatexis were temporally related. The development of in situ dating methods that can overcome certain limitations of conventional methods (e.g., Harrison et al., 1995a, 1997a) produced results that challenged this widely held assumption of Himalayan tectonics and suggest to us a rather different history for the region (e.g., Harrison et al., 1998b).

In this paper, we summarize the petrological, geochronological, and structural constraints on the evolution of the Himalayan range and describe recent developments which indicate that the inverted metamorphic sequences formed during Late Miocene slip along the MCT and is thus unrelated to Early Miocene recrystallization and anatexis above the thrust. This recognition leads to our favored model (i.e., Harrison et al., 1998b), which we describe in this

* Corresponding author.

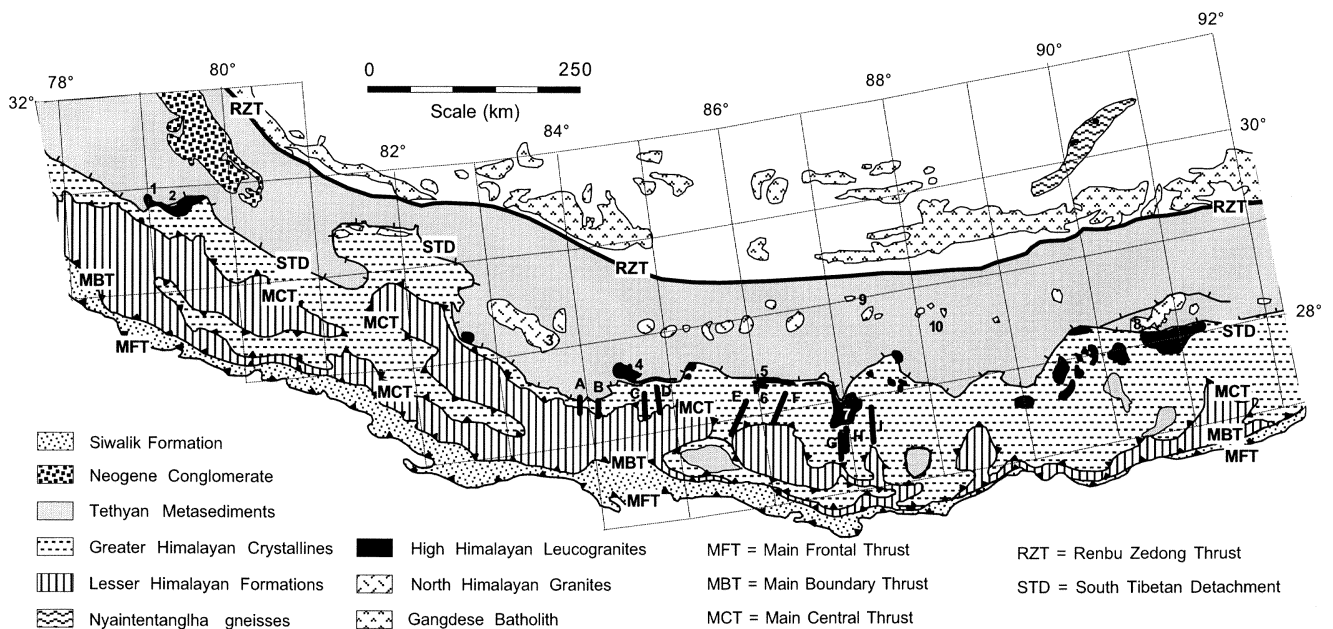


Fig. 1. Geological map of the Himalaya and Southern Tibet. Ages for granites identified by numeral are obtained from U–Th–Pb monazite dates. Sources of data are: (1) Gangotri: 22.4 ± 0.5 Ma, Harrison et al. (1997b); (2) Shivling: 21.9 ± 0.5 Ma, Harrison et al. (1997b); (3) Manaslu: 22.9 ± 0.6 Ma (Larkya La phase), 19.3 ± 0.3 Ma (Bintang phase), Harrison et al. (1999); (4) Makalu: 23 ± 1 Ma; Schärer (1984); (5) Shisha Pangma: 20.2 ± 0.2 Ma and 17.3 ± 0.3 Ma, Searle et al. (1997); (6) Nyalam: 17.2 ± 0.9 Ma; Schärer et al. (1986); (7) Gonto-La: 12.5 ± 0.5 Ma, Edwards and Harrison (1997); (8) Dolpo: 17.6 ± 0.3 Ma, Harrison et al. (1999); (9) Lhagoi Kangri: 15.1 ± 0.5 Ma, Schärer et al. (1986); (10) Maja: 9.5 ± 0.5 , Schärer et al. (1986); (11) Zaskar (not shown): 20.0 ± 0.5 Ma, Noble and Searle (1995). Location of thermobarometry transects detailed in Fig. 3 are indicated by letters A through I.

paper in some detail, that appears to reconcile the new timing constraints with the large pool of knowledge gained from earlier geophysical measurements and the rock record. We then return to previously proposed

models to evaluate the extent to which they are consistent with current geologic evidence. In general, we find that many of these hypotheses are either incompletely supported by, or inconsistent with, the recently

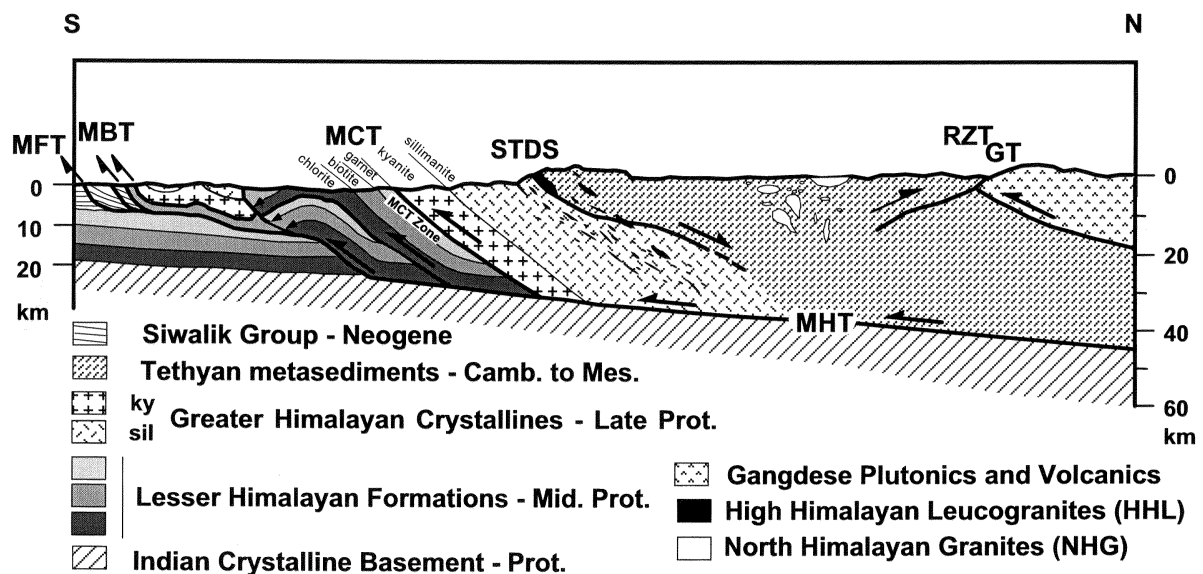


Fig. 2. Generalized cross section through the central Himalaya illustrating the juxtaposition of the major lithostratigraphic units across the major Himalayan faults, inverted metamorphism, and plutonic belts (modified from Schelling and Arita (1991) and Zhao et al. (1993)). See Fig. 1 for key to abbreviations for faults.

derived timing constraints. The picture that emerges from this review is of continuous Himalayan convergence being manifested as episodic phenomena (e.g., out-of-sequence thrusting, intermittent magmatism) while creating geological relationships with a high potential for imparting misleading clues (e.g., juxtaposition of anatectic rocks against apparent inverted metamorphic sequences).

2. Review of Himalayan geology

2.1. Indo-Asian collision

Because of the initially irregular continental margins of India and southern Asia, the period between their first contact and final suturing was undoubtedly protracted. Sedimentological evidence indicates that the northwest tip of India had collided with Asia at ~50 Ma (e.g., Le Fort, 1996; Rowley, 1996) and both continents appear to have met along the full length of a ~3000 km long suture by about 40 Ma (Dewey et al., 1988). Paleomagnetic evidence indicates that the Indo-Australian plate has moved northward by 2600 ± 900 km relative to the Eurasian plate since this time (Dewey et al., 1989; Le Pichon et al., 1992). In that same interval, southern Tibet moved north with respect to Eurasia by 2000 ± 600 km (Besse and Courtillot, 1988) suggesting something less than 1000 km underthrusting of India beneath Asia.

Immediately prior to the onset of the Indo-Asian collision, the northern boundary of the Indian shield was likely a thinned margin on which Proterozoic clastic sediments and the Cambrian–Eocene Tethyan shelf sequence were deposited (Le Fort, 1996). South-directed thrusts within the Himalaya, including the MCT, Main Boundary Thrust (MBT), and the Main Frontal Thrust (MFT) (Gansser, 1964; Bouchez and Pêcher, 1981; Arita, 1983; Le Fort, 1986; Burbank et al., 1996) appear to sole into a common decollement, the Main Himalayan Thrust (MHT) (Zhao et al., 1993; Nelson et al., 1996; Brown et al., 1996). In general, the MCT places high grade gneisses of Indian origin, the Greater Himalayan Crystallines (GHC), on top of the Lesser Himalayan Formations (LHF), comprised largely of intermediate grade schists and phyllites. The protoliths of the Lesser Himalayan Formations and Greater Himalayan Crystallines are interpreted, respectively, to be Middle and Late Proterozoic clastic rocks (Parrish and Hodges, 1996). Dating studies (e.g., Parrish and Hodges, 1996; Vance and Harris, 1999) suggest that high grade metamorphism first affected the protolith of the Greater Himalayan Crystallines during an Early Tertiary, or Eohimalayan, phase of crustal thickening (Le Fort, 1996). The MBT juxtaposes schists of the Lesser

Himalayan Formations against unmetamorphosed Miocene–Pleistocene molasse (Siwalik Group), and the MFT is presently active within Quaternary sediments. Estimates of the amount of slip along the MHT based on balanced cross section reconstruction's (Schelling, 1992; Srivastava and Mitra, 1994; DeCelles et al., 1998) are consistent with a displacement of about 500 km.

The Greater Himalayan Crystallines are juxtaposed against lower-grade Tethyan shelf deposits by the South Tibetan Detachment System (STDS) (see Figs. 1 and 2). Although it is widely assumed that slip on the STDS and MCT occurred at least in part simultaneously (Burchfiel et al., 1992; Hodges et al., 1992; Searle et al., 1997), no evidence has yet been documented requiring such a relationship (cf. Vance et al., 1998). Constraints on the timing of thrusting along the MCT are that its hanging wall was deforming at ~22 Ma (Hodges et al., 1996; Coleman, 1998) and a broad shear zone below the GHC was active between about 8–4 Ma (Harrison et al., 1997a). Brittle faulting within the MCT hanging wall at *ca* 3 Ma has also been reported (e.g., Macfarlane, 1993). It is generally assumed, but not certain, that the MCT was inactive during the Middle Miocene development of the MBT (Burbank et al., 1996). Whether or not slip along the MCT overlapped with displacement on the STDS is uncertain. The clearest constraint on the timing of displacement along the STDS is that the exposed detachment fault near Gonto-La (Fig. 1) was active at 12.4 ± 0.4 Ma (Edwards and Harrison, 1997). Although extensional structures cut by the Manaslu intrusive complex (Guillot, 1993) must be older than 23–19 Ma (Harrison et al., 1999), the relationship of the STDS to this body remains uncertain. Reports that the STDS north of Mt. Everest is cross-cut by an Early Miocene granite (Hodges et al., 1992; Harrison et al., 1995a) have proven to be in error (Murphy and Harrison, 1999), probably due to a sampling mishap. The ages of ductilely deformed granite sills in this area are consistent with Middle Miocene slip on the STDS (Schärer et al., 1986; Hodges et al., 1998; Murphy and Harrison, 1999).

2.2. Inverted metamorphism

The juxtaposition of the Greater Himalayan Crystallines and Lesser Himalayan Formations across the MCT is associated at most locations in the Himalaya with an increase in metamorphic grade with higher structural position (i.e., shallower depth) (Figs. 2 and 3). The Greater Himalayan Crystallines vary substantially in thickness across the Himalaya. For example, hanging wall thickness increases from about 2 km in the Kali Gandaki to 20 km in central Bhutan, probably due to (1) variable initial thickness, (2) the

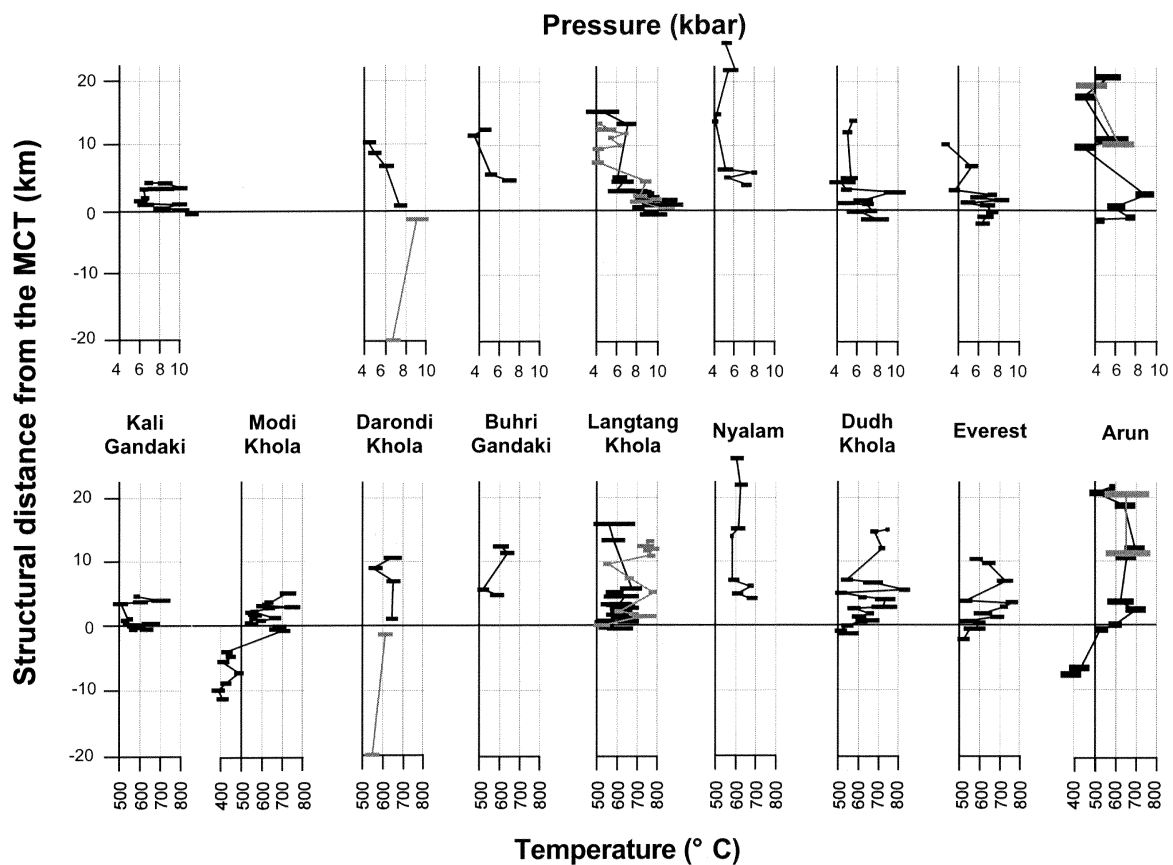


Fig. 3. Distribution of pressures and temperatures calculated from mineral equilibria versus structural distance from the MCT for samples collected along transects indicated on Fig. 1. Sources for the data shown are as follows: A, Kali Gandaki River (Hodges et al., 1996); B, Modi Khola (Kaneko, 1995); C, Darondi Khola, grey (Catlos et al., 1997), black (Hodges et al., 1988); D, Burhi Gandaki (Hodges et al., 1988), E, Langtang, grey (Inger and Harris, 1992), black (Macfarlane, 1995); F, Nyalam (Hodges et al., 1993); G, Dudh Kosi (Hubbard, 1989); H, Everest (Hubbard, 1989); I, Arun, black (Pognante and Benna, 1993), grey (Brunel and Kienast, 1986). In general, pressures within the Greater Himalayan Crystallines decrease from 6–8 kbar at the MCT to values of 3–4 kbars close to the STDS. Temperatures within both the Greater Himalayan Crystallines and Lesser Himalayan Formations tend to be ~600–700°C at the MCT but vary widely elsewhere.

MCT cutting up section at certain locations, and (3) imbrication within the MCT hanging wall. In the central Himalaya, where the structural thickness of the Greater Himalayan Crystallines is typically 8–12 km, the inverted metamorphic section reaches sillimanite grade (Fig. 2). Thermobarometric studies of the Greater Himalayan Crystallines indicate a general decrease in pressure with increasing distance above the MCT (Fig. 3). Typically, pressures of 7–8 kbar were achieved adjacent to the MCT (kyanite grade), whereas peak pressures at the structurally highest levels were only about 3–4 kbar (sillimanite grade). Metamorphism within the Lesser Himalayan Formations (Fig. 2) increases from zeolite to kyanite grade over a north–south distance of ~20 km. The region approximately bounded by the garnet isograd in the Lesser Himalayan Formations and the hanging wall gneisses of the Greater Himalayan Crystallines is typically characterized by a highly sheared, 4–8 km thick zone of distributed deformation with a top-to-

the-south shear sense, referred to as the ‘MCT Zone’ (Fig. 2). Note that this definition is distinct from the question of whether an inverted metamorphic field gradient exists within the MCT hanging wall at certain locations (e.g., Davidson et al., 1997).

2.3. Himalayan leucogranites

An apparently unique feature of the Himalayan range is the presence of two roughly parallel granite belts, the High Himalayan leucogranites (HHL) and the North Himalayan granites (NHG) (Fig. 1). The High Himalayan leucogranites form a discontinuous chain of sills exposed adjacent to the STDS (Fig. 1). Magmatic temperatures have been estimated at *ca* 700–750°C (Montel, 1993). The North Himalayan granite belt runs parallel to, and ~80 km to the north of, the High Himalaya and is composed of about one and a half dozen generally elliptical-shaped plutons. Exposed plutons of the northern belt appear in general

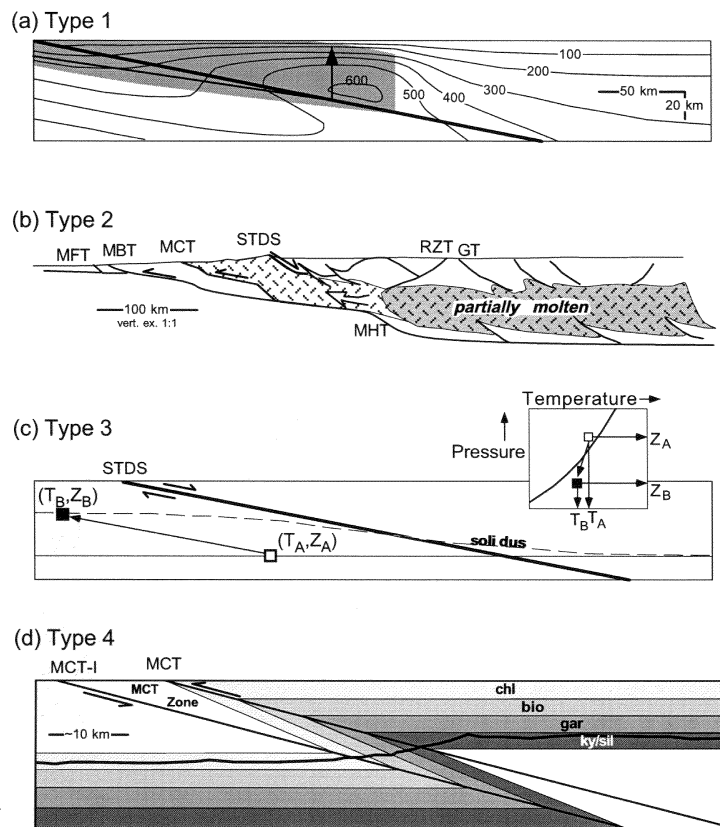


Fig. 4. Schematic illustrations of the four different models proposed to explain the relationship of inverted metamorphism and/or anatexis to large-scale faulting within the Himalaya. (a) Type 1: Inverted metamorphism developed within the footwall of the MCT and anatexis in the hanging wall are spatially and temporally related by thrusting. This illustration, modified from Huerta et al. (1996), shows an inverted metamorphic geotherm forming as a result of the transfer of radiogenic crust from the footwall of a subduction zone to the hanging wall. The direction of material transport is shown by the line with the arrowhead, and the shaded region corresponds to crust accreted to the hanging wall. Isotherms are shown in °C. (b) Type 2: Thrusting results from anatexis. The illustration shows the interpretation of Nelson et al. (1996) of a partially molten Tibetan middle crust that is being actively extruded southward. In this interpretation, the Greater Himalayan Crystallines is an earlier extruded equivalent. (c) Type 3: Anatexis results from normal faulting. This figure illustrates the change in the depth–temperature conditions in the footwall of a normal fault. The initial depth, Z_A , is associated with temperature T_A . Following slip on the normal fault, the depth is substantially reduced to Z_B , but the effect of heat advection results in only minor cooling to temperature T_B . If (Z_A, T_A) is immediately above the solidus of a vapor absent equilibrium (e.g., muscovite dehydration melting), the passage to (Z_B, T_B) induces partial melting (see inset). (d) Type 4: Apparent inverted metamorphism in the footwall of the MCT is produced by deformation of two right-way-up metamorphic sequences. This illustration, modified from Hubbard (1996), shows the effect of deforming a normal metamorphic sequence across a broad shear zone. Note that for the topography shown (solid curve), the bedrock exposure corresponds to a monotonic, left to right, increase in metamorphic grade.

to have been intruded at relatively shallow depths into the Tethyan cover rocks and well above the STDS (Le Fort, 1986). They differ from the HHL in their emplacement style (Figs. 1 and 2) and possibly higher melting temperatures ($> 750^\circ\text{C}$), suggested by non-eutectic compositions and high light rare earth contents coupled with low monazite inheritance (Debon et al., 1986; Schärer et al., 1986; Montel, 1993; Harrison et al., 1997b).

Assessment of the crystallization age of Himalayan granites is complicated by the minimum melt character of these magmas. Heterogeneous $^{87}\text{Sr}/^{86}\text{Sr}$ and $^{143}\text{Nd}/^{144}\text{Nd}$ initial ratios (e.g., Le Fort et al., 1987) have, with rare exception (Deniel et al., 1987), precluded whole rock isochron dating. $^{40}\text{Ar}/^{39}\text{Ar}$ dating

of Himalayan granite or their contact aureoles yield either *ca* 15–19 Ma cooling ages or older dates which reflect contamination by excess ^{40}Ar (e.g., Copeland et al., 1990; Guillot et al., 1994; Harrison and Mahon, 1995). U–Pb dating of zircon and monazite are complicated by the low solubilities of these phases in leucogranite magmas (Harrison and Watson, 1983; Montel, 1993), the likelihood of their containing an inherited component (Copeland et al., 1988), and the possibly of U loss from monazite (R. Parish, personal communication, 1999). Igneous monazites commonly incorporate significant ^{230}Th during crystallization resulting in the production of unsupported $^{206}\text{Pb}^*$. However, $^{208}\text{Pb}/^{232}\text{Th}$ ion microprobe dating of monazite does not suffer from problems of disequilibrium Pb^* and

the high spatial resolution of the measurement method generally permits the question of homogeneity of calculated ages to be explicitly examined. What we consider to be the reliable crystallization ages of Himalayan leucogranites, many of which are derived from recent ion microprobe Th–Pb monazite dates, are enumerated in the caption of Fig. 1. Plutons from the High Himalayan leucogranite belt vary in age from 24.0 to 17.2 Ma, but most the large granite bodies comprising the majority of the leucogranite were emplaced during two pulses at 23 ± 1 Ma and 19 ± 1 Ma (Harrison et al., 1998b). Crystallization ages for granites we assign to the North Himalayan belt range from 17.6 to 9.5 Ma. Note, however, that classifying Himalayan granites into two discrete belts may be misleading in that temporally contiguous, northward propagating melting (Harrison et al., 1997b) could produce spatially discontinuous patterns due to variable exposure.

2.4. Models relating inverted metamorphism, anatexis, and faulting

A variety of models have been proposed to explain the relationship of inverted metamorphism and/or anatexis to large-scale faulting within the Himalaya (Fig. 4). Models that assume that anatexis and inverted metamorphism are spatially and temporally related to each other and result from slip on the Himalayan thrust system include melting induced by thermal relaxation following nappe emplacement accompanied by fluid influx from the subducting footwall (e.g., Le Fort, 1975), frictional heating during thrusting (e.g., Arita, 1983; Molnar and England, 1990; England et al., 1992; England and Molnar, 1993), radioactive heating alone or combined with other sources under prolonged deep crustal residence (e.g., Molnar et al., 1983), and accretion of highly radioactive crust to the MCT hanging wall coupled with high denudation (e.g., Royden, 1993; Huerta et al., 1996). The origin of the North Himalayan granites has not been so inextricably tied to the development of Himalayan faulting, but their relative youth has been ascribed to a low rate of fluid infiltration across the MCT (Le Fort, 1986) and heat focusing by thermal refraction off low thermal conductivity Tethyan metasediments (Pinet and Jaupart, 1987). The second type of model proposes that thrusting within the Himalaya is caused by melting rather than vice versa. In this view, regions of the crust thermally weakened by melting are the locus of deformation the leads to large-scale faulting (e.g., Bird, 1978; Nelson et al., 1996; Davidson et al., 1997). While these models generally do not propose mechanisms for the origin of inverted metamorphism, Bird (1978) did allow for the possibility that preexisting isograds had been recumbently folded (e.g., Frank et al.,

1973). A third class of models also makes no predictions regarding the development of inverted metamorphism but proposes that anatexis is due to decompression resulting from slip on the STDS rather than to thrusting (e.g., Harris and Massey, 1994). The fourth model type is primarily concerned with the inverted metamorphism and assumes no causal relationship between anatexis and faulting. These models infer that the distribution of metamorphic assemblages resulted from subsequent deformation (e.g., Hubbard, 1996). We return to these models later to assess their compatibility with recently derived constraints described below.

3. Recent developments

3.1. Inverted metamorphism

Despite the common assumption of a causal link between anatexis and inverted metamorphism across the MCT, the timing of recrystallization of the Lesser Himalayan Formation rocks in the MCT footwall had not, until very recently, been directly dated. Harrison et al. (1997a) utilized the observation that detrital monazite is generally destabilized in pelitic rocks during diagenesis but reappears under lower amphibolite grade conditions (e.g., Kingsbury et al., 1993) to establish the timing of garnet-grade metamorphism affecting the Lesser Himalayan Formations in the central Himalaya. Allantite is the principal host of LREE in the Lesser Himalayan Formations schists at chlorite and biotite grades, but reacts to form monazite near the garnet isograd ($\sim 500^\circ\text{C}$). Using the $^{208}\text{Pb}/^{232}\text{Th}$ ion microprobe method (Harrison et al., 1995a), monazite grains, including one encompassed by a mm-sized garnet, were dated at 5.6 ± 0.2 Ma. Thermobarometry indicates that garnet growth occurred at a P – T of 6–8 kbar and $550 \pm 30^\circ\text{C}$. As the garnet and monazite isograds are nearly coincident in temperature (i.e., $\sim 500^\circ\text{C}$; Kingsbury et al., 1993), Harrison et al. (1997a) concluded that garnet growth in the presently exposed rocks occurred at a depth of ~ 25 km at ~ 6 Ma. Additional Th–Pb monazite dating in the Lesser Himalayan Formations from the central and Garhwal Himalaya (Catlos et al., 1997, 1999) all yield Late Miocene ages, indicating that this recrystallization event was widespread across the Himalaya. K–Ar mica ages from N–S transects across these regions decrease from 20–16 Ma in the upper MCT hanging wall to 6–3 Ma within and adjacent to the MCT Zone (Hubbard and Harrison, 1989; Copeland et al., 1991; Metcalfe, 1993).

Assuming that slip along the MCT had terminated during the Early Miocene, Harrison et al. (1997a) explained the pattern of geochronological results as

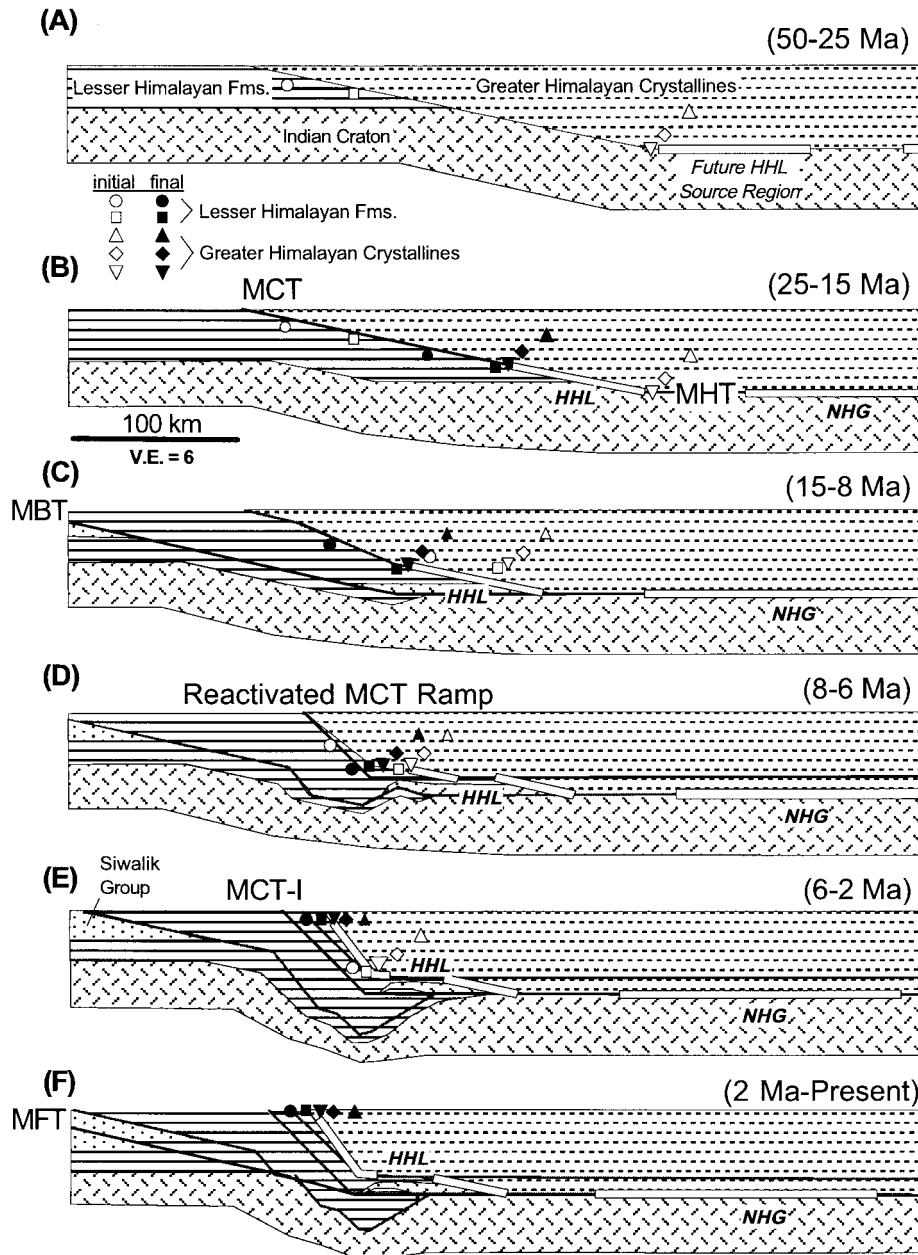


Fig. 5. Schematic illustration of tectonic development of the Himalayan thrust system (vertical exaggeration 6:1). Active faults are shown as bold black lines while abandoned faults are indicated with bold gray lines. Symbols shown correspond to sample positions described in detail in Harrison et al. (1997a, 1998b). Open and closed symbols indicate initial and final positions for the time interval shown. (a) Possible 25 Ma distribution of the protoliths of Greater Himalayan Crystallines (GHC) and Lesser Himalayan Formations (LHF) with respect to Indian cratonic margin after Eohimalayan thickening from *ca* 50–25 Ma. Future site of the High Himalayan leucogranite (HHL) source region is shown at 25 Ma. (b) Thrusting along the Main Himalayan Thrust (MHT) flat and Main Central Thrust (MCT) decollement from 25–15 Ma. Note that this fault system forms immediately above refractory rocks of the Indian craton. (c) Thrusting along MHT flat and MBT ramp from 15–8 Ma. Abandonment of the MCT ramp at 15 Ma causes accretion of upper LHF rocks to the hanging wall. (d) Out-of-sequence thrusting in the high Himalaya from 8–6 Ma involving upper LHF (approximately equivalent to reactivated MCT thrust ramp). (e) Activation of MCT-I and further development of MCT Zone (6–2 Ma) leads to accretion of lower LHF rocks to hanging wall. (f) Abandonment of the MCT zone at 2 Ma. Southward transfer of displacement to MFT ramp/MHT decollement. Present predicted positions of HHL and North Himalayan Granite (NHG) source regions are shown by regions shaded white.

due to thrust reactivation during the Late Miocene. A break back from the MBT to the MCT, presumed to have steepened as a result of post-Early Miocene deformation (Fig. 5d), could reflect a stress increase in the hinterland resulting from an increase in elevation of the Tibetan Plateau during the Late Miocene (Harrison et al., 1995b) or readjustment of the thrust wedge following significant erosional and/or tectonic denudation of the hanging wall (Dahlen, 1984). Early Miocene slip along the MCT emplaced gneisses of the Greater Himalayan Crystallines over the Lesser Himalayan Formations along an initially well-defined fault resulting in burial metamorphism of the latter. After a period of either inactivity or slip at relatively low rates during the Middle Miocene, renewed deformation resulted in development of the broad underlying MCT shear zone during the Late Miocene, and ultimately accretion of metamorphosed rocks of the Lesser Himalayan Formations to the hanging wall during Late Miocene–Early Pliocene time. In this view, the inverted metamorphism within this portion of the Himalaya largely reflects tectonic juxtaposition of two temporally unrelated, right-way-up metamorphic sequences. Results of numerical modeling (Harrison et al., 1997a) demonstrated that isotopic and petrologic constraints are met by assuming that the MCT fault reactivated at 8 Ma with a slip rate of about 20 mm/yr, followed by activation of the MCT Zone and accretion of garnet grade Lesser Himalayan Formations rocks between 6–4 Ma. While the thermal evolution of the MCT zone predicted by this model satisfies both the Th–Pb age results from monazite inclusions preserved within garnet and the observed distribution of K–Ar mineral ages (Harrison et al., 1997a), it remains possible that reactivation of the MCT ramp initiated somewhat earlier than *ca* 8 Ma, or that it remained active (e.g., Henry and Copeland, 1999) at reduced rates throughout the Middle Miocene.

3.2. Origin of the two Himalayan leucogranite belts

One of the principal implications of the recognition that recrystallization of the MCT footwall is a Late Miocene phenomenon, and thus not temporally related to production of the Early Miocene High Himalayan leucogranites, is that anatexis of the Greater Himalayan Crystallines need not be restricted to the MCT ramp (cf. England et al., 1992). Harrison et al. (1997b) explored an alternative model that ascribed the spatial and temporal variations of granite emplacement to continuous slip on a shallow dipping decollement that cuts through crust previously metamorphosed during the Eohimalayan phase (Le Fort, 1996) of collision. They assumed that, immediately prior to collision, the northern Indian margin re-

sembled Fig. 5a, and that during the Eohimalayan stage, the Greater Himalayan Crystallines protolith underwent high grade recrystallization and anatexis (see Pêcher, 1989; Hodges et al., 1994, 1996; Parrish and Hodges, 1996; Edwards and Harrison, 1997; Coleman, 1998; Vance and Harris, 1999). As a consequence, metamorphism and anatexis in the Greater Himalayan Crystallines protolith would produce a stratified paragenetic sequence in which dehydration and partial melting reactions caused grade to increase regularly with depth (Harrison et al., 1997b).

The 2-D thermal evolution models of Harrison et al. (1997b) demonstrated that a shear stress of 30 MPa along a shallow dipping fault that cuts through a metamorphically stratified crust is sufficient to produce two horizontally separated granite belts. Assuming that the present-day Himalayan convergence rate of 20 mm/yr (Billham et al., 1997) is appropriate to the period 24–10 Ma, the model predicted that a phase of anatexis would begin almost immediately, provided that the thermal structure developed during the Eohimalayan phase had not significantly decayed. Refrigeration of the shear zone near the fault ramp, coupled with the propagation of the melting front toward the ramp, causes the first predicted phase of melting to cease at \sim 20 Ma. A second phase of melting begins when temperature exceeds the higher temperature melting reaction at 18 Ma and continues until 12 Ma. Model predictions regarding horizontal separation of the belts, their age contrast and emplacement styles appear to broadly accord with observation.

3.3. A unified model for Himalayan metamorphism and anatexis

The generally good match between geologic observation and predictions of the models proposed for the origin of the inverted metamorphic sequences (Harrison et al., 1997a) and the two granite belts (Harrison et al., 1997b) demonstrated the physical plausibility of these mechanisms, but stops well short of constituting conclusive evidence of their validity. In fact, evaluating each of these models in isolation provides an unjustifiable degree of freedom — i.e., the temperature distribution and structural development predicted by the two granite model at *ca* 8 Ma should be consistent with initial conditions of the model which successfully predicts the pattern and age of inverted metamorphism. This problem can be further constrained by incorporating estimates of the total amount of slip along the MHT over the past 25 Ma. This requirement, and the recognition that the earlier models had incorporated an overly simplistic melting model (Harrison et al., 1997b) and geothermal structure (Harrison et al., 1997a), led Harrison et al. (1998b) to link the model for generation of the paired

granite belts with the development of the inverted metamorphic sequences. They adopted the assumption of Harrison et al. (1997b) that footwall rocks underlying the basal decollement consisted of refractory Indian basement that was not susceptible to partial melting at the temperatures $<760^{\circ}\text{C}$, which has the effect of limiting anatexis to hanging wall rocks overlying the basal decollement.

Harrison et al. (1998b) were able to take advantage of several recent advances in understanding of the structure of the collision zone to further constrain boundary conditions, model variables, and aspects of the geometric evolution of the Himalaya. The general structural framework was based on results of seismic reflection profiling in southern Tibet which show the Himalayan thrusts soling into a shallow ($\sim 9^{\circ}$) dipping decollement (Zhao et al., 1993; Nelson et al., 1996; Brown et al., 1996). The magnitude of shortening within the Greater Himalayan Crystallines, Lesser Himalayan Formations, and Sub-Himalaya have recently been estimated from balanced cross sections (e.g., Schelling, 1992; Srivastava and Mitra, 1994) that suggest that about half of the *ca* 1000 km of shortening between the Indian Shield and southern Tibet (Chen et al., 1993; Patzelt et al., 1996) has been absorbed within the Himalaya. Geodetic measurements indicate that the present convergence rate across the Himalaya is 20 ± 1 mm/yr (Bilham et al., 1997). The timing of activation of the MBT and MFT are broadly known (Schelling and Arita, 1991; Burbank et al., 1996) and the age of both granite belts and recrystallization of the MCT footwall are reasonably well known (Harrison et al., 1997a,b).

The model of Harrison et al. (1998b) also employs a ramp-flat geometry to simulate crustal thickening and assumes that the initiation of the Himalayan thrust system was localized at the boundary between the Greater Himalayan Crystallines and the Indian craton. The slip history they utilized is schematically depicted in Fig. 5. Thrusting begins after the crust has been thickened in response to ~ 25 m.y. of Eohimalayan crustal shortening (Fig. 5a) and proceeds at a constant slip rate of 20 mm/yr. The resulting 250 km of shortening in the hanging wall is accommodated as follows: slip occurs on the MHT/MCT ramp between 25–15 Ma (Fig. 5b), on the MHT/MBT ramp between 15–8 Ma (Fig. 5c), and on the MHT and various fault ramps defining the MCT zone between 8–2 Ma (Fig. 5d–f).

Using a shear stress of 30 MPa, Harrison et al. (1998b) calculated the amount of heat produced by dissipation and partitioned this thermal energy between heating the rocks and melting. They described melt production by an experimentally-determined relationship for melt fraction as a function of temperature appropriate for an intercalated sequence of

muscovite-rich (relatively fertile) and plagioclase-poor (relatively infertile) lithologies (e.g., Gardien et al., 1995).

The assumption that the onset of partial melting does not appreciably lower rock shear strength is fundamental to the Harrison et al. (1998b) model. This behavior is indicated when dislocation creep is the dominant mechanism and strain rate is low relative to the rate of melt migration. Studies of texturally equilibrated materials indicate that plastic deformation can squeeze excess melt from the rock leaving the deformation rate essentially unaffected (e.g., Dell'Angelo and Tullis, 1988; Rushmer, 1996). At strain rates appropriate to Himalayan convergence across a narrow shear zone (e.g., 10^{-11} to 10^{-12} /s) and temperatures of $\sim 750^{\circ}\text{C}$, shear stress values of approximately 10 MPa are predicted from empirical flow laws for both partially molten (e.g. Rutter, 1997) and solid quartzo-feldspathic materials (e.g., Stüwe and Sandiford, 1994).

The restricted time interval over which low-temperature melting occurs in the Harrison et al. (1998b) model agrees well with observed span of HHL ages. Although HHL ages vary from 24–17 Ma, the majority of the melt was produced at 23 ± 1 Ma (Harrison et al., 1998b). Moreover, the agreement of model predictions with the known crystallization ages of North Himalayan granites (17–10 Ma) is equally good. The apparent success in matching the apparent separation distance between the HHL and NHG of approximately 80 km (Fig. 1) is the direct result of an arbitrary assumption regarding the position of the ramp/flat and the prior history of Eohimalayan melting. The volume of magma calculated by the model is broadly consistent with the $\sim 3\%$ exposure of leucogranites in the Himalaya (Le Fort et al., 1987) and the physical attributes of the two magmatic belts agree reasonably well with the melting model of Harrison et al. (1998b). For example, the relatively viscous melts produced in the lower temperature melting reaction (*ca* 740°C) are consistent with the emplacement of the HHL as syntectonic sills and dikes rather than diapirs. The magmas formed by the higher temperature reactions ($>760^{\circ}\text{C}$) predicted for the NHG are reasonably expected to be sufficiently buoyant and thermally energetic to ascend as diapirs into the middle crust, consistent with the character of the NHG belt. The ramp-flat model is consistent with the observation that the Greater Himalayan Crystallines immediately above the present exposure of the MCT (Fig. 5f) did not experience temperatures high enough to cause widespread melting (Barbey et al., 1996). Migmatization higher up section may reflect imbrication of the Greater Himalayan Crystallines (e.g., Davidson et al., 1997), the advection of magmatic heat associated with leucogranite emplacement into shallower crustal levels, or a

nearly isothermal middle crust (e.g., Hodges et al., 1988) in which the geotherm is steeper than the dP/dT slope of the melting reaction. With respect to this latter point, the available thermobarometric data (Fig. 3) and transition from kyanite to sillimanite with increasing structural position appear inconsistent with the existence of inverted metamorphism in the Greater Himalayan Crystallines, at least within the central Himalaya.

Harrison et al. (1998b) found that varying certain model parameters could dramatically effect predicted melting histories. For example, small differences in initial temperature distribution (10's of °C) significantly altered calculated melt volumes, and reducing the flow stress within the shear zone below 10 MPa essentially eliminated melting due to biotite breakdown and forestalled initial melting at locations appropriate to the HHL for several million years. In contrast, the effect of increasing the dimensions of the shear zone in the model permits the melting of increasingly larger volumes of rock.

Temperature–time histories and peak pressures and temperatures predicted by the Harrison et al. (1998b) model as a function of structural distance from the MCT generally agree reasonably well with measured values. In addition to producing kinematic and thermal histories consistent with the available thermochronology and geothermometry for the MCT zone, the fault–bend–fold geometry employed in the Harrison et al. (1998b) model also accounts for the observed variations of metamorphic conditions within the MCT hanging wall (e.g., Hodges et al., 1988). Thermobarometric results from the MCT hanging wall indicate that shallower crustal levels are exposed to the north. Such paleobarometric variation is consistent with rotation produced by the fault–bend–fold geometry (Ruppel and Hodges, 1994; Harrison et al., 1997a) and indicates an apparent lithostatic gradient of ~ 0.27 kbar/km within the hanging wall (Hodges et al., 1988).

4. Evaluation of evolutionary models linking deformation, magmatism, and metamorphism

The spectacular nature of the mountain belt containing the highest peaks on our planet has drawn a tremendous amount of interest to Himalayan geology. Despite this attention, we caution that what is learned from the Himalayan range may possess limited value as a general model for orogeny. For example, the pattern of crustal displacements in response to the Indo-Asian collision is inconsistent with simple permutations of end-member tectonic mechanisms (e.g., Indian or Asian underthrusting, continental injection, mantle delamination, delayed underplating, orogenic collapse, lateral extrusion, intra-arc thickening), but

instead requires a complex, time-dependent transfer among several of these processes, often with multiple mechanisms operating simultaneously (Kong et al., 1997; Harrison et al., 1998a). The tremendous amount of attention that has been directed at understanding the petrologic evolution of the Himalaya belies the fact that the two mechanisms most often called upon to produce crustal melting, footwall anatexis following overthrusting (e.g., England and Thompson, 1984) and underplating of mafic magma (e.g., Huppert and Sparks, 1988), have rarely been invoked to explain Himalayan anatexis (cf. Bird, 1978). Furthermore, signature geologic features of the Himalaya appear to be unique to that range. For example, we are unaware of any other mountain range that contains parallel belts of leucogranites of contrasting age. Although our goal in understanding the tectonic development of the Himalaya cannot be to develop a general model for direct export to other mountain belts, recovering details of the geologic evolution should permit us to better understand what factors control changes in tectonic regime.

The models that have been advanced to explain the relationship of inverted metamorphism and/or anatexis to large-scale faulting within the Himalaya are characterized by their originality and ingenuity. However, several can clearly be seen to fail tests of their predictions in light of recent observations. In this section, we critically examine the four general groups of models of Himalayan petrogenesis: (1) inverted metamorphism developed within the LHF and anatexis of the GHC are spatially and temporally related by thrusting; (2) thrusting results from GHC anatexis; (3) GHC anatexis results from normal faulting; and (4) apparent inverted metamorphism in the LHF is produced by deformation of two right-way-up metamorphic sequences.

4.1. Type 1: Anatexis and inverted metamorphism are spatially and temporally related by thrusting

Type 1 models assume a causal relationship between anatexis within the Greater Himalayan Crystallines and the inverted metamorphic sequence (Fig. 4a). The general requirement of these models is an extraordinary source of heat to maintain high temperatures in the GHC to permit melting while Indian underthrusting cools the hanging wall from below. Although most type 1 models thus share a common flaw (i.e., the underlying assumption that anatexis and the exposed inverted metamorphic sequences are temporally related), aspects of the processes they invoke may be applicable to originally contiguous, though now widely spaced, footwall and hanging wall rocks of the Himalayan thrust system.

The first modern type 1 model was Le Fort's (1975)

proposal that thermal relaxation following thrusting along the MCT heated the footwall sufficiently to induce dehydration reactions. When these fluids were introduced into the still hot hanging wall, they fluxed the gneisses producing the leucogranite melts. Anticipating that this mechanism alone was not capable of creating a lateral thermal gradient high enough to create the apparent inverted metamorphism while maintaining hanging wall temperatures sufficient for anatexis to occur, Le Fort (1975) introduced shear heating to this role. As noted above, the fact that GHC melting and LHF recrystallization in the presently exposed section are not temporally related obviates the need for high hanging wall temperatures during thrusting along the ramp. Furthermore, the necessity of introducing fluids to produce conditions appropriate for melting has been challenged on at least two grounds. Harris et al. (1993) noted that the high Rb/Sr ratios of Himalayan leucogranites relative to their assumed GHC source rocks precludes water-saturated melting and instead favors muscovite dehydration melting (e.g., Thompson, 1982). Specifically, the comparatively small proportion of Rb-rich mica relative to Sr-rich feldspar consumed in water-saturated melting could not produce elevated Rb/Sr ratios whereas modally more significant breakdown of muscovite during dehydration melting has the potential to do so. Moreover, recent experimental results show that water-saturated melting of Himalayan source rocks under likely crustal conditions yield melts of trondhjemitic composition (Patiño Douce and Harris, 1998) that are unlike the leucogranite compositions observed.

The basic elements of the Le Fort (1975) model (i.e., synchronicity of anatexis and inverted metamorphism, fluid-present melting, shear heating) were subsequently adopted by numerous workers, but perhaps no more enthusiastically than by Phillip England and his co-workers who developed this problem quantitatively in a series of papers extending over 17 years (e.g., Graham and England, 1976; Molnar and England, 1990; England et al., 1992, England and Molnar, 1993). The argument stressed in these papers is that the observed thermal structure requires shear stresses along the MCT in the range 100–1100 MPa (England and Molnar, 1993). These values, however, appear to far exceed an upper bound for ductile shearing of a few 10's of MPa inferred from paleopiezometry (e.g., Engelder, 1993), laboratory deformation experiments (e.g., Rutter, 1997), or tectonic modeling (e.g., Kong and Bird, 1996). Moreover, relative to the wet melting conditions they assumed, even higher shear stresses would be required to create conditions suitable for vapor absent melting of metapelitic source rocks.

Other workers who were critical of the requirement that extraordinarily high shear stresses (i.e., ≥ 100

MPa) be maintained in hydrated crustal rocks at liquidus temperatures (e.g., Bird, 1978; Molnar et al., 1983), but who nonetheless accepted a causal link between melting and inverted metamorphism, sought other possible sources of heat to explain Himalayan petrogenesis. One possible heat source, suggested by the relatively high U and Th concentrations of the Himalayan gneisses, is radioactivity. Molnar et al. (1983) explored this avenue and found that, coupled with the generally high heat flow inferred for northern India (e.g., Rao et al., 1976; cf. Gupta, 1993), radioactive heat generation of several $\mu\text{W}/\text{m}^3$ could create conditions conducive to melting after several ten's of millions of years of continental subduction. Royden (1993) examined the steady-state effect of accreting highly radioactive material from an accretionary prism to the hanging wall of a subduction zone under conditions of rapid erosion and concluded that this scenario could explain Himalayan anatexis and the apparent inverted geothermal structure. Huerta et al. (1996) further investigated the time-dependent effects of erosion and accretion of heat producing elements on the thermal structure of orogenic systems. They directly compared the results of the model following 32 m.y. of evolution to the MCT thrust zone and concluded that this scenario may have exerted a first order control on the thermal and metamorphic evolution of the Himalayan orogen. Henry et al. (1997) adopted the main elements of the Royden (1993) model with an emphasis on understanding the effect of the thermal structure on Himalayan topography. Limitations of these continuous accretion–erosion models, such as the predication of widespread exposure of rocks from depths far greater than recognized, can be circumvented by addition of a thrust flat in the model (e.g., Henry and Copeland, 1999). However, in addition to the unsupported assumption that a high (*ca* 5°C/km) horizontal thermal gradient was maintained on the MCT ramp during the Early Miocene, implications of this variant of the type 1 model (i.e., Royden, 1993; Huerta et al., 1996, 1998; Henry et al., 1997) appear inconsistent with two fundamental characteristics of Himalayan anatexis; the synchronous appearance of the voluminous HHL magmas and their isotopic character.

The large plutons of the Garhwal, Manaslu, and Makalu regions, which comprise the majority of leucogranite exposed along the western and central High Himalaya (Le Fort et al., 1987), appear to have been emplaced at 23 ± 1 Ma (Schärer, 1984; Harrison et al., 1997b). No older plutons of comparable size have been documented. Given that ten's of millions of years are required by the radiogenic heating/rapid erosion mechanism to create conditions suitable for melting, this model would appear not to predict the synchronous appearance of melting across the collision front.

Such behavior is more consistent with a mechanism that produces localized thermal anomalies, such as shear heating.

The second potential weakness of the radiogenic heating/rapid erosion model (e.g., Royden 1993; Huerta et al., 1996) is the requirement that significant material transfer occur from the footwall of the Himalayan thrust to the hanging wall. As described earlier, the MCT marks the boundary between the Middle Proterozoic Lesser Himalayan Formations and Late Proterozoic Greater Himalayan Crystallines. These two rock types can be clearly distinguished on the basis of detrital zircon ages (Parrish and Hodges, 1996) and isotopic composition (Deniel et al., 1987; Derry and France-Lanord, 1996). For example, the Lesser Himalayan Formations are characterized by an average $^{87}\text{Sr}/^{86}\text{Sr} \approx 1.1$ whereas the Greater Himalayan Crystallines range only from 0.73–0.78 (France-Lanord and Le Fort, 1988; Guillot, 1993). Had lower plate rocks continuously accreted to the MCT hanging wall, the distinctive isotopic character of the LHF and GHC, as well as the granites derived from the GHC, would not be expected to persist to the present. While this specific objection precludes the large-scale addition of material to the hanging wall from the LHF, the general principle of the model may still be valid (i.e., accretion coupled with rapid erosion is restricted to within the GHC).

Although radioactive heat generation has also been suggested as a contributing cause for the melting of the North Himalayan granites (e.g., Pinet and Jaupart, 1987), this proposal is not subject to the timing constraints imposed by the 23 ± 1 Ma age of the HHL nor does it involve accretion of LHF material.

4.2. Type 2: Himalayan thrusting is caused by melting

In contrast to type 1, this class of model proposes that thrusting within the Himalaya is caused by heating/melting rather than being a consequence of it. Bird (1978) argued that mantle lithosphere delamination beneath the Himalaya was a plausible consequence of continental collision. One effect of delamination would be to uplift the crust immediately above the region where the mantle lithosphere had been removed. This in turn would create a large strain at the edge of the delaminated region making it a likely site for formation of a large-scale thrust. As asthenospheric heat diffuses upward, the thrust propagates into the newly weakened crust. Although Bird (1978) showed quantitatively that this model could produce sufficient heat to produce synchronous anatexis and inverted metamorphism over a period of 5–10 Ma, it is now clear that crustal melting and metamorphism in the exposed MCT footwall occurred at widely separated times (Harrison et al., 1997a).

On the basis of seismic reflection profiling along a southern Tibetan graben, Nelson et al. (1996) advocated a reversal of roles for thrusting and anatexis. They interpreted bright spot anomalies beneath the Yadong–Gulu rift as indicating that the Tibetan middle (15–20 km) crust is partially molten, and speculated that the region between the MCT and STDS is the earlier extruded equivalent (Fig. 4b). The variation in age among the Himalayan granites is interpreted to reflect a semi-continuous record of this partially molten, mid-crustal layer. The Nelson et al. (1996) model requires temperatures sufficient for muscovite dehydration melting (i.e., $\sim 750^\circ\text{C}$; Harris and Inger, 1992) at a depth of 15 km, but, because the seismogenic mantle beneath southern Tibet is constrained to be $\sim 750^\circ\text{C}$ (Ruppel and McNamara, 1997), the crust would have to be essentially isothermal. The generally high heat flow (Francheteau et al., 1984) and upper crustal residence of the Curie isotherm (Nelson et al., 1999) in southern Tibet are both consistent with elevated temperatures within the middle crust. The existence of anomalously warm conditions beneath southern Tibet throughout the Miocene and persisting until present-day appears to be explicable by the previously described continuous accretion–erosion models. For example, the nearly isothermal structure required by the Nelson et al. (1996) model from 15 km depth to the base of the crust is similar to that predicted at 20 Ma for the seemingly reasonable case of a convergence rate of 15 mm/yr, an erosion rate of 1 mm/yr, and a radioactive heat production of $2.5 \mu\text{W}/\text{m}^3$ (Henry et al., 1997). However, this model requires uniformly rapid erosion from a region equivalent to the ~ 200 -km-wide zone between the trace of the Himalayan thrust system and the Indus Tsangpo suture. Moreover, the model geometry predicts increasingly deep levels of exposure to the north. In fact, the level of exposure throughout the vast majority of this region is greenschist grade with only minor amounts (< 15 km) of post-Oligocene exhumation indicated for much of this area (e.g., Ratschbacher et al., 1994). The deep crustal exposures are largely restricted to the GHC, which forms a rather narrower (i.e., 5–100 km wide) aperture than required by the Henry et al. (1997) model and occurs at the opposite side of the wedge (i.e., to the south) than predicted. The fact that the Tethyan sediments have not been completely removed from atop the heat producing element enriched Indian supracrustal section represents a severe shortcoming of this model.

The model of Nelson et al. (1996) has been challenged on several fronts. Makovsky and Klemperer (1999) concluded that the bright spots do not represent melts, but rather regions containing on the order of 10% aqueous fluids. Owens and Zandt (1997) found that the seismic velocity structure and magnitude of

Poisson's ratio beneath southern Tibet indicate a generally cold crust and explained this as due to the underthrusting of the Indian craton beneath southern Tibet. The broadly coherent stratigraphy within the GHC (Le Fort, 1996) appears inconsistent with the extrusion model of Nelson et al. (1996). Basement rocks uplifted on the flank of the Yadong–Gulu rift are in essence a window into the Tibetan middle crust. While this terrane contains leucogranites that were intruded immediately prior to the initiation of detachment faulting at ~ 8 Ma, reconnaissance-scale observations are not suggestive of widespread, in situ partial melting at that time (Pan and Kidd, 1992; Harrison et al., 1995b; D'Andrea et al., 1999). Isotopic tracers from these Middle Miocene granitoids indicate the presence of a *ca* 2 Ga component (D'Andrea et al., 1999), in contrast to the protolith of crustal melts from elsewhere in the Lhasa Block which are characterized by *ca* 1 Ga neodymium model ages (Harris et al., 1988).

Lincoln Hollister and his co-workers (e.g., Swapp and Hollister, 1991; Hollister, 1993; Davidson et al., 1997) have emphasized the role of anatexis in localizing strain to approximately doubly thicken the GHC in the Bhutan Himalaya. Davidson et al. (1997) concluded that the advection of heat by thrusting and syntectonic migration of leucogranites from the base of the GHC contributed to the formation of an inverted metamorphic field gradient within the MCT hanging wall. While possibly valid for the Bhutan region, structural elements unique to that region (e.g., the Kakhtang thrust, > 20 km thickness of the GHC) (Gansser, 1964) may restrict their model from being generalized to much of the rest of the Himalaya.

4.3. Type 3: Himalayan anatexis results from decompression melting during slip along the STDS

A third class of model (Fig. 4c) links anatexis directly to decompression melting related to slip on the STDS rather than to thrusting (e.g., Harris et al., 1993), although the development of the STDS may ultimately be a response to thickening via the various splays of the MHT (e.g., Burg et al., 1984). This model is superficially attractive because of the positive dP/dT of vapor absent equilibria, particularly for reactions involving muscovite, coupled with the large vertical displacement inferred across the STDS (Burchfiel et al., 1992).

Nigel Harris and his co-workers (e.g., Harris and Inger, 1992; Harris et al., 1993; Harris and Massey, 1994; Patiño Douce and Harris, 1998) used a variety of approaches, including trace element modeling and experimental petrology, to establish that most Himalayan anatexis occurred by fluid absent reactions rather than via water-saturated melting. This view has subsequently been widely accepted (e.g., Guillot and

Le Fort, 1995; Searle et al., 1997; Davidson et al., 1997; Harrison et al., 1998b). However, the correlative proposal of Harris and co-workers that muscovite dehydration melting was triggered in the Himalaya by tectonic decompression rather than by heating appears problematic to us for the following reasons: (1) the extremely rapid and large magnitude denudation that are required by the minor effect that decompression has on melting likely source rock compositions; (2) the difficulty of producing multiple anatectic phases via decompression; and (3) the lack of definitive timing constraints linking slip on the STDS with anatexis.

The depth dependence of muscovite dehydration melting in the lower crust of $\sim 3.7^\circ\text{C}/\text{km}$ (Huang and Wyllie, 1973) is small relative to the geotherm expected at these depths ($\sim 15\text{--}20^\circ\text{C}/\text{km}$). Biotite dehydration is even less of a factor since dP/dT slopes of relevant breakdown equilibria are even steeper. Consequently, decompression melting is a relatively inefficient process when compared to anatexis on a thrust flat driven by modest dissipative heating (Harrison et al., 1998b). For example, to produce a melt fraction of rock by decompression melting comparable to that resulting from 1 m.y. of subhorizontal 20 mm/a slip (Bilham et al., 1997) at 30 MPa shear stress requires ~ 30 km of denudation over 1 m.y. (Harrison et al., 1999). The effect produced by slower denudation is negligible. For example, Harrison et al. (1998b) found that incorporating a denudation rate characteristic of that documented for the Himalaya (~ 1 mm/a; e.g., Henry et al., 1997) into a model evaluating the conditions required for melting along an MHT-type thrust ramp (see Zhao et al., 1993) did not perceptibly increase the melt fraction.

Episodic melting by decompression is particularly problematic. Recently, several studies have documented cases of protracted anatexis at certain locations in the Himalaya (e.g., Searle et al., 1997; Harrison et al., 1999). Harrison et al. (1999) assessed the feasibility of decompression melting in producing the two pulses of magmatism at 23 ± 1 and 19 ± 1 Ma documented to have built the Manaslu intrusive complex. Using a numerical thermal model, they calculated P – T – t paths in the footwall source region at horizontal distances of 5, 10, and 20 km from a normal fault dipping at 30° . After introducing a pressure dependence to Harrison et al.'s (1998b) melting model, they found that while a 10% initial melt could be obtained for source regions located > 10 km from the fault given a slip rate of 20 mm/yr (i.e., a 10 mm/yr denudation rate), lower slip rates or positions closer to the normal fault did not result in conditions appropriate to melting. For locations far from the fault, it was found that an initial, rapid decompression followed relatively shortly thereafter by a second, similarly rapid pulse of exhumation could create temporally distinct melting episodes. For

example, a vertical component of slip of 10, 2.5 and 10 mm/yr for the time intervals 0–1, 1–3 and 3–4 m.y., respectively, produces two melting phases separated by 4 m.y. However, the extreme (and improbable) denudation rates required by the model to produce the two temporally distinct melting episodes would create widespread exposure of rocks originating from 10–12 kbar depths. Such high pressure assemblages are not recognized within or adjacent to the Manaslu intrusive complex (Fig. 3), in the nearby HHC gneisses, or, with minor exceptions, elsewhere in the Himalayan range.

In addition, timing constraints that definitively link slip on the STDS with anatexis are lacking. Presently, there is little direct evidence that the STDS was active between 24–19 Ma when the majority of the HHL formed. Although earlier reports from north of Mt. Everest indicated otherwise (e.g., Hodges et al., 1992; Harrison et al., 1995a), the timing of ductile deformation related to the STDS is only constrained to have occurred in the interval 17–14 Ma (Schärer et al., 1986; Hodges et al., 1998; Murphy and Harrison, 1999).

4.4. Type 4: Inverted metamorphism is due to transposition of right-way-up metamorphic sequences

A few investigators have emphasized the role of retrograde transposition of a normally zoned metamorphic sequence to create the inverted pattern of isograds developed beneath the MCT (Fig. 4d). Models have been proposed that involve ductile folding of pre-existing isograds (Searle and Rex, 1989; Grujic et al., 1996), imbricate thrusting (Arita, 1983; Brunel and Kienast, 1986), and ductile shearing of an existing zone right-way-up metamorphic sequence (Hubbard, 1996). Although each of these mechanisms can explain the creation of an apparent inverted metamorphic sequence, this category of models has generally been viewed as either inconsistent with geological constraints (e.g., Pêcher, 1989) or of limited importance (e.g., England et al., 1992). Field relations alone have not been able to select between model types 1 and 4 and, until recently, no dating method had been developed capable of establishing the timing of footwall recrystallization.

Although the above mentioned mechanisms stand apart from type 1 models in rejecting the role of the hanging wall as heat source in producing the inverted metamorphic sequences, they have also tended to assume that peak metamorphism recorded in the hanging wall and footwall occurred simultaneously. The recognition that recrystallization of the MCT footwall is a Late Miocene phenomenon (Harrison et al., 1997a), and thus not temporally related to production of the Himalayan leucogranites, and the corollary that Greater Himalayan Crystalline anatexis need not be

restricted to the MCT ramp, has largely removed the need for exceptional heat sources as proposed by type 1 models. While essentially all models described above can explain the generation of leucogranite in the hanging wall, none can account for hanging wall anatexis and footwall metamorphism being separated in time by more than 10–15 Ma (e.g., Harrison et al., 1997a; Catlos et al., 1997, 1999). As described in the previous section, this requirement led us (Harrison et al., 1998b) to propose that inverted metamorphism within the footwall was created and later juxtaposed against the granite source region in the hanging wall.

A rather different approach was taken by Jamieson et al. (1996) who proposed a mechanism by which an apparent inverted metamorphic sequence could be produced in the absence of an inverted crustal isotherm. Their model assumes a highly specific geometry in which the orogen is characterized by a strain singularity at the point where the subducting mantle lithosphere detaches from the thickening crust. This configuration produces two symmetrical, oppositely dipping, intra-crustal thrusts referred to as the pro- and retroshear zones. One consequence of crustal thickening in this geometry is the tectonic juxtaposition of widely differing initial positions that reach peak metamorphic grade at varying times and locations within the orogen. Jamieson et al. (1996) compared model predictions with P – T data from the MCT zone of central Nepal and concluded that an inverted crustal thermal gradient was not required to explain the inverted metamorphic sequence which instead could result from differential horizontal transport and exhumation of deep-seated metamorphic rocks. They did not specifically address the origin of crustal melting or the fate of the Indian lithosphere that previously underlay the Himalaya.

Jamieson et al. (1996) acknowledge that their model challenges conventional wisdom in positing the MCT as a retroshear of opposing vergence to that of the subduction zone, usually assumed to be south-directed as India thrusts beneath southern Asia. Rather, they suggest that the Asian mantle was subducted beneath India during the period in which they assumed the MCT zone formed. Although their model is provocative in showing how an inverted metamorphic sequence could be dynamically created in the absence of an inverted crustal geotherm, we have significant reservations regarding their view of its application to the Himalaya. First, we question whether present geologic and geophysical data are compatible with either subduction geometry. Seismic evidence appears to support a north-dipping Moho beneath the Himalaya (e.g., Nelson et al., 1996; Owens and Zandt, 1997; Henry et al., 1997). Although the Jamieson et al. (1996) model does predict diachronous peak metamorphism, the pattern is inconsistent with the bimodal timing constraints

(Harrison et al., 1997a) that have been brought to light subsequently. Although Jamieson et al. (1996) do not offer candidates for the pro-shear in a central Himalayan context, the Renbu–Zedong Thrust (Fig. 2) has the appropriate geometry. However, present timing constraints (Quidelleur et al., 1997) suggest that it was inactive between 24–18 Ma and 8–4 Ma when the MCT is known to have accommodated significant displacement (Hodges et al., 1996; Coleman, 1998; Harrison et al., 1997a).

5. Summary

A tremendous amount of information that is fundamental to understanding the Neogene tectonic and petrogenetic evolution of the Himalaya has become available over the past several years. Constraints derived from these investigations include: (1) the protoliths of the Lesser Himalayan Formations and Greater Himalayan Crystallines are, respectively, Middle and Late Proterozoic clastic rocks that first underwent high grade metamorphism during the Eohimalayan phase of collision; (2) deformation was occurring in the presently exposed hanging wall of the MCT ramp during the Early Miocene; (3) the major phase of leucogranite magmatism in the High Himalayan belt occurred by dehydration melting between 24–22 Ma; (4) recrystallization within the inverted metamorphic sequences exposed in the MCT footwall occurred between 8–4 Ma; (5) the Himalayan thrust faults all sole into a shallow dipping decollement termed the Main Himalayan Thrust (MHT); (6) a minimum of ~250 km of post-collision slip was been accommodated along the MHT; and (7) the present rate of convergence across the Himalaya is 20 ± 1 mm/yr.

The numerous models that have been advanced to explain the relationship of inverted metamorphism and/or anatexis to large-scale faulting within the Himalaya fall into four general groups: (1) inverted metamorphism developed within the footwall of the MCT and anatexis in the hanging wall are spatially and temporally related by thrusting; (2) thrusting results from anatexis; (3) anatexis results from normal faulting; and (4) apparent inverted metamorphism in the footwall of the MCT is produced by deformation of two right-way-up metamorphic sequences. We have revisited these various proposals in light of the recently derived constraints described above and found most to be seriously flawed, in many cases because the assumption that inverted metamorphism and anatexis are synchronous is incorrect. The hypothesis that best appears to explain all observations is a variant of the type (4) model in which continuous convergence is manifested by episodic magmatism and out-of-sequence thrusting.

Acknowledgements

This research was sponsored by grants from the National Science Foundation. We thank Professors Le Fort and Upreti for inviting this contribution, and Nigel Harris, Leigh Royden and Peter Bird for helpful reviews.

References

- Arita, K., 1983. Origin of the inverted metamorphism of the Lower Himalaya, central Nepal. *Tectonophysics* 95, 43–60.
- Barbey, P., Brouand, M., LeFort, P., Pêcher, A., 1996. Granite-migmatite genetic link: the example of the Manaslu granite and Tibetan Slab migmatites in central Nepal. *Lithos* 38, 63–79.
- Besse, J., Courtillot, V., 1988. Paleogeographic maps of the continents bordering the Indian Ocean since the Early Jurassic. *Journal of Geophysical Research* 93, 11,791–11,808.
- Bilham, R., Larson, K., Freymueller, J., Project Idylhim members, 1997. GPS measurements of present-day convergence across the Nepal Himalaya. *Nature* 386, 61–64.
- Bird, P., 1978. Initiation of intracontinental subduction in the Himalaya. *Journal of Geophysical Research* 83, 4975–4987.
- Bouchez, J.L., Pêcher, A., 1981. Himalayan Main Central Thrust pile and its quartz-rich tectonites in central Nepal. *Tectonophysics* 78, 23–50.
- Brown, L.D., Zhao, W., Nelson, K.D., Hauck, M., Alsdorf, D., Ross, A., Cogan, M., Clark, M., Liu, X., Che, J., 1996. Bright spots, structure, and magmatism in Southern Tibet from INDEPTH seismic reflection profiling. *Science* 274, 1688–1691.
- Brunel, M., Kienast, J.R., 1986. Étude pétro-structurale des chevauchements ductiles himalayens sur la transversale de L'Everest-Makalu (Népal oriental). *Canadian Journal of Earth Sciences* 23, 1117–1137.
- Burbank, D.W., Beck, R.A., Mulder, T., 1996. The Himalayan foreland basin. In: Yin, A., Harrison, T.M. (Eds.), *The Tectonics of Asia*. Cambridge University Press, New York, pp. 149–188.
- Burchfiel, B.C., Chen, Z., Hodges, K.V., Liu, Y., Royden, L.H., Deng, C., Xu, J., 1992. The South Tibetan Detachment System, Himalayan Orogen: Extension contemporaneous with and parallel to shortening in a collisional mountain belt. *Geological Society of American Special Paper* 269, 41.
- Burg, J.P., Brunel, M., Gapais, D., Chen, G.M., Liu, G.H., 1984. Deformation of leucogranites of the crystalline Main Central Sheet in southern Tibet (China). *Journal of Structural Geology* 6, 535–542.
- Catlos, E.J., Harrison, T.M., Grove, M., Lovera, O.M., Yin, A., Kohn, M.J., Ryerson, F.J., Le Fort, P., Upreti, B.N., 1997. Further evidence for Late Miocene reactivation of the Main Central Thrust (Nepal Himalaya) and the significance of the MCT-I. *EOS* 78, 543.
- Catlos, E.J., Harrison, T.M., Searle, M.P., Hubbard, M., 1999. Evidence for Late Miocene Reactivation of the Main Central Thrust: From Garhwal to the Nepali Himalaya. In: 14th Himalaya-Karakorum-Tibet Workshop, Abstract volume, Kloster Ettal, Germany, pp. 20–22.
- Chen, Y., Courtillot, V., Cogne, J.P., Besse, J., Yang, Z., Enkin, R., 1993. The configuration of Asia prior to the collision of India: Cretaceous paleomagnetic constraints. *Journal of Geophysical Research* 98, 21,927–21,941.
- Coleman, M.E., 1998. U-Pb constraints on Oligocene-Miocene deformation and anatexis within the central Himalaya, Marsyandi valley, Nepal. *American Journal of Science* 298, 553–571.
- Copeland, P., Parrish, R.R., Harrison, T.M., 1988. Identification of

- inherited radiogenic Pb in monazite and its implications for U-Pb systematics. *Nature* 333, 760–763.
- Copeland, P., Harrison, T.M., Le Fort, P., 1990. Age and cooling history of the Manaslu granite: Implications for Himalayan tectonics. *Journal of Volcanology and Geothermal Research* 44, 33–50.
- Copeland, P., Harrison, T.M., Hodges, K.V., Maréjoul, P., Le Fort, P., Pêcher, A., 1991. An Early Pliocene thermal perturbation of the Main Central Thrust, Central Nepal: Implications for Himalayan tectonic. *Journal of Geophysical Research* 96, 8475–8500.
- Dahlen, F.A., 1984. Noncohesive critical coulomb wedges: An exact solution. *Journal of Geophysical Research* 89, 10,125–10,133.
- D'Andrea, J., Harrison, T.M., Grove, M., 1999. The thermal and physical state of the South Tibetan middle crust Between 20–8 Ma: U-Th-Pb and Nd isotopic evidence from the Nyainqentanglha Massif. In: 14th Himalaya-Karakorum-Tibet Workshop, Abstract volume, Kloster Ettal, Germany, pp. 29–30.
- Davidson, C., Grujic, D.E., Hollister, L.S., Schmid, S.M., 1997. Metamorphic reactions related to decompression and synkinematic intrusion of leucogranite, High Himalayan Crystallines, Bhutan. *Journal of Metamorphic Geology* 15, 593–612.
- Debon, F., Le Fort, P., Sheppard, S.M.F., Sonet, J., 1986. The four plutonic belts of the Transhimalaya-Himalaya: A chemical, mineralogical, isotopic, and chronological synthesis along a Tibet-Nepal section. *Journal of Petrology* 21, 219–250.
- DeCelles, P.G., Gehrels, G.E., Quade, J., Ojha, T.P., Kapp, P.A., Upreti, B.N., 1998. Neogene foreland basin deposits, erosional unroofing, and the kinematic history of the Himalayan fold-thrust belt, western Nepal. *Geological Society of America Bulletin* 110, 2–21.
- Dell'Angelo, L.N., Tullis, J., 1988. Experimental deformation of partially molten granitic aggregates. *Journal of Metamorphic Geology* 6, 495–515.
- Deniel, C., Vidal, P., Fernandez, A., Le Fort, P., Peucat, J.J., 1987. Isotopic study of the Manaslu granite (Himalaya, Nepal): inferences on the age and source of the Himalayan leucogranites. *Contributions to Mineralogy and Petrology* 96, 78–92.
- Derry, L.A., France-Lanord, C., 1996. Neogene Himalayan weathering history and river $^{87}\text{Sr}/^{86}\text{Sr}$: impact on the marine Sr record. *Earth and Planetary Science Letters* 142, 59–74.
- Dewey, J.F., Shackelton, R.M., Chang, C., Sun, Y., 1988. The tectonic evolution of the Tibetan Plateau. *Philosophical Transactions of the Royal Society of London* A327, 379–413.
- Dewey, J.F., Cande, S., Pitman, W.C., 1989. Tectonic evolution of the India-Eurasia collision zone. *Ecologiae Geologica Helvetica* 82, 717–734.
- Edwards, M.A., Harrison, T.M., 1997. When did the roof collapse? Late Miocene N-S extension in the High Himalaya revealed by Th-Pb monazite dating of the Khula Kangri granite. *Geology* 25, 543–546.
- Engelder, T., 1993. In: *Stress regimes in the lithosphere*. Princeton University Press, Princeton, NJ 457 pp.
- England, P.C., Thompson, A.B., 1984. Pressure-temperature-time paths of regional metamorphism, Part I: Heat transfer during the evolution of regions of thickened continental crust. *Journal of Petrology* 25, 894–928.
- England, P., Molnar, P., 1993. The interpretation of inverted metamorphic isograds using simple physical calculations. *Tectonics* 12, 145–157.
- England, P., Le Fort, P., Molnar, P., Pêcher, A., 1992. Heat sources for Tertiary metamorphism and anatexis in the Annapurna-Manaslu region, Central Nepal. *Journal of Geophysical Research* 97, 2107–2128.
- France-Lanord, C., Le Fort, P., 1988. Crustal melting and granite genesis during the Himalayan collision orogenesis. *Transactions of the Royal Society of Edinburgh: Earth Science* 79, 183–196.
- Francheteau, J., Jaupart, C., Xian, J.S., Wen-Hua, K., De-Lu, L., Jia-Cha, B., Hun-Pin, W., Hsia-Yeu, D., 1984. High heat flow in southern Tibet. *Nature* 307, 32–36.
- Frank, W., Hoinkes, G., Miller, C., Purtscheller, F., Richter, W., Thöni, M., 1973. Relations between metamorphism and orogeny in a typical section of the Indian Himalayas. *Tschermaks Mineralogische und Petrographische Mitteilungen* 20, 303–332.
- Gansser, A., 1964. *The Geology of the Himalayas*. Wiley-Interscience, New York.
- Gardien, V., Thompson, A.B., Grujic, D., Ulmer, P., 1995. Experimental melting of biotite + plagioclase \pm muscovite assemblages and implications for crustal melting. *Journal of Geophysical Research* 100, 15,581–15,591.
- Graham, C.M., England, P.C., 1976. Thermal regimes and regional metamorphism in the vicinity of overthrust faults: an example of shear heating and inverted metamorphic zonations from southern California. *Earth and Planetary Science Letters* 31, 142–152.
- Grujic, D., Casey, M., Davidson, C., Hollister, L.S., Kundig, R., Pavlis, T., Schmid, S., 1996. Ductile extrusion of the Higher Himalayan Crystalline in Bhutan — Evidence from quartz microfabrics. *Tectonophysics* 260, 21–43.
- Guillot, S., 1993. Le granite du Manaslu (Nepal Central) marqueur de la subduction et de l'extension intracontinentales Himalayennes. *Géologie Alpine* 19, 1–97.
- Guillot, S., Le Fort, P., 1995. Geochemical constraints on the bimodal origin of High Himalayan leucogranites. *Lithos* 35, 221–234.
- Guillot, S., Hodges, K.V., Le Fort, P., Pêcher, A., 1994. New constraints on the age of the Manaslu leucogranite: Evidence for episodic tectonic denudation in the central Himalaya. *Geology* 22, 559–562.
- Gupta, M.L., 1993. Is the Indian Shield hotter than other Gondwana Shields. *Earth and Planetary Science Letters* 115, 275–285.
- Harris, N., Inger, S., 1992. Trace element modelling of pelite derived granites. *Contributions to Mineralogy and Petrology* 110, 45–56.
- Harris, N., Massey, J., 1994. Decompression and anatexis of Himalayan metapelites. *Tectonics* 13, 1537–1546.
- Harris, N., Inger, S., Massey, J., 1993. The role of fluids in the formation of High Himalayan leucogranites. In: Searle, M.P., Treloar, P.J. (Eds.), *Himalayan Tectonics*, Geological Society of London Special Publication, 74, 391–400.
- Harris, N.B.W., Xu, R., Lewis, C.L., Hawkeworth, C.J., Zhang, Y., 1988. Isotope geochemistry of the 1985 Tibet Geotraverse, Lhasa to Golmud. *Philosophical Transactions of the Royal Society of London* A327, 263–285.
- Harrison, T.M., Watson, E.B., 1983. Kinetics of zircon dissolution and zirconium diffusion in granitic melts of variable water content. *Contributions to Mineralogy and Petrology* 84, 66–72.
- Harrison, T.M., Mahon, K.I., 1995. New constraints on the age of the Manaslu leucogranite: Evidence for episodic tectonic denudation in the central Himalaya: Comment. *Geology* 23, 478–479.
- Harrison, T.M., McKeegan, K.D., Le Fort, P., 1995a. Detection of inherited monazite in the Manaslu leucogranite by $^{208}\text{Pb}/^{232}\text{Th}$ ion microprobe dating: Crystallization age and tectonic significance. *Earth and Planetary Science Letters* 133, 271–282.
- Harrison, T.M., Copeland, P., Kidd, W.S.F., Lovera, O.M., 1995b. Activation of the Nyainqentanglha shear zone: implications for uplift of the southern Tibetan Plateau. *Tectonics* 14, 658–676.
- Harrison, T.M., Ryerson, F.J., Le Fort, P., Yin, A., Lovera, O.M., Catlos, E.J., 1997a. A Late Miocene-Pliocene origin for the Central Himalayan inverted metamorphism. *Earth and Planetary Science Letters* 146, E1–E8.
- Harrison, T.M., Lovera, O.M., Grove, M., 1997b. New insights into the origin of two contrasting Himalayan granite belts. *Geology* 25, 899–902.
- Harrison, T.M., Yin, A., Ryerson, F.J., 1998a. Orographic evolution of the Himalaya and Tibet. In: Crowley, T.J., Burke, K. (Eds.),

- Tectonic Boundary Conditions for Climate Reconstructions. Oxford University Press, New York, pp. 39–72.
- Harrison, T.M., Grove, M., Lovera, O.M., Catlos, E.J., 1998b. A model for the origin of Himalayan anatexis and inverted metamorphism. *Journal of Geophysical Research* 103, 27,017–27,032.
- Harrison, T.M., Grove, M., McKeegan, K.D., Coath, C.D., Lovera, O.M., Le Fort, P., 1999. Origin and episodic emplacement of the Manaslu intrusive complex, Central Himalaya. *Journal of Petrology* 40, 3–19.
- Henry, P., Copeland, P., 1999. Thermal and kinematic models for central Nepal: Persistence of a decollement-ramp-decollement system throughout the Miocene. *Journal of Conference Abstracts* 4, 49.
- Henry, P., Le Pichon, X., Goffe, B., 1997. Kinematic, thermal and petrological model of the Himalayas: Constraints related to metamorphism within the underthrust Indian crust and topographic elevation. *Tectonophysics* 273, 31–56.
- Hodges, K.V., Bowring, S., Davidek, K., Hawkins, D., Krol, M., 1988. Evidence for rapid displacement on Himalayan normal faults and the importance of tectonic denudation in the evolution of mountain ranges. *Geology* 26, 483–486.
- Hodges, K.V., Parrish, R.R., Housh, T.B., Lux, D.R., Burchfiel, B.C., Royden, L.H., Chen, Z., 1992. Simultaneous Miocene extension and shortening in the Himalayan orogen. *Science* 258, 1466–1470.
- Hodges, K.V., Burchfiel, B.C., Royden, L.H., Chen, Z., Liu, Y., 1993. The metamorphic signature of contemporaneous extension and shortening in the central Himalayan orogen: Data from the Nyalam transect, southern Tibet. *Journal of Metamorphic Geology* 11, 721–737.
- Hodges, K.V., Hames, W.E., Olszewski, W.J., Burchfiel, B.C., Royden, L.H., Chen, Z., 1994. Thermobarometric and $^{40}\text{Ar}/^{39}\text{Ar}$ geochronologic constraints on Eohimalayan metamorphism in the Dinggy area, southern Tibet. *Contributions to Mineralogy and Petrology* 117, 151–163.
- Hodges, K.V., Parrish, R.R., Searle, M.P., 1996. Tectonic evolution of the central Annapurna Range, Nepalese Himalayas. *Tectonics* 15, 1264–1291.
- Hodges, K.V., Le Fort, P., Pêcher, A., 1998. Possible thermal buffering by crustal anatexis in collisional orogens: Thermobarometric evidence from the Nepalese Himalaya. *Geology* 16, 707–710.
- Hollister, L.S., 1993. The role of melt in the uplift and exhumation of orogenic belts. *Chemical Geology* 108, 31–48.
- Huang, W.L., Wyllie, P.J., 1973. Melting relations of muscovite-granite to 35 kbar as a model for fusion of metamorphosed subducted oceanic sediments. *Contributions to Mineralogy and Petrology* 42, 1–14.
- Hubbard, M.S., 1989. Thermobarometric constraints on the thermal history of the Main Central Thrust Zone and Tibetan Slab, eastern Nepal Himalaya. *Journal of Metamorphic Geology* 7, 19–30.
- Hubbard, M.S., 1996. Ductile shear as a cause of inverted metamorphism: example from the Nepal Himalaya. *Journal of Geology* 104, 493–499.
- Hubbard, M.S., Harrison, T.M., 1989. $^{40}\text{Ar}/^{39}\text{Ar}$ age constraints on deformation and metamorphism in the MCT Zone and Tibetan Slab, eastern Nepal Himalaya. *Tectonics* 8, 865–880.
- Huerta, A.D., Royden, L.H., Hodges, K.V., 1996. The interdependence of deformational and thermal processes in mountain belts. *Science* 273, 637–639.
- Huerta, A.D., Royden, L.H., Hodges, K.V., 1998. The thermal structure of collisional orogens as a response to accretion, erosion, and radiogenic heating. *Journal of Geophysical Research* 103, 15,287–15,302.
- Huppert, H.E., Sparks, R.S.J., 1988. The generation of granitic magmas by intrusion of basalt into continental crust. *Journal of Petrology* 29, 599–624.
- Inger, S., Harris, N.B.W., 1992. Tectonothermal evolution of the High Himalayan Crystalline sequence, Langtang Valley, northern Nepal. *Journal of Metamorphic Geology* 10, 439–452.
- Jamieson, R.A., Beaumont, C., Hamilton, J., Fullsack, P., 1996. Tectonic assembly of inverted metamorphic sequences. *Geology* 24, 839–842.
- Kaneko, Y., 1995. Thermal structure in the Annapurna region, central Nepal Himalaya: Implication for the inverted metamorphism. *Journal of Mineralogy, Petrology and Economic Geology* 90, 143–154.
- Kingsbury, J.A., Miller, C.F., Wooden, J.L., Harrison, T.M., 1993. Monazite paragenesis and U-Pb systematics in rocks of the eastern Mojave Desert, California, U.S.A.: implications for thermochronometry. *Chemical Geology* 110, 147–168.
- Kong, X., Bird, P., 1996. Neotectonics of Asia: thin-shell, finite-element models with faults. In: Yin, A., Harrison, T.M. (Eds.), *The Tectonics of Asia*. Cambridge University Press, New York, pp. 18–35.
- Kong, X., Yin, A., Harrison, T.M., 1997. Evaluating the role of pre-existing weakness and topographic distributions in the Indo-Asian collision by use of a thin-shell numerical model. *Geology* 25, 527–530.
- Le Fort, P., 1975. Himalayas, the collided range: Present knowledge of the continental arc. *American Journal of Science* 275A, 1–44.
- Le Fort, P., 1986. Metamorphism and magmatism during the Himalayan collision. In: Coward, M.P., Ries, A.C. (Eds.), *Collision Tectonics*, Geological Society of London Special Publication, 19, 159–172.
- Le Fort, P., 1996. The Himalayan evolution. In: Yin, A., Harrison, T.M. (Eds.), *The Tectonics of Asia*. Cambridge University Press, New York, 95–109.
- Le Fort, P., Cuney, M., Deniel, C., France-Lanord, C., Sheppard, S.M.F., Upreti, B.N., Vidal, P., 1987. Crustal generation of the Himalayan leucogranites. *Tectonophysics* 134, 39–57.
- Le Pichon, X., Fournier, M., Jolivet, L., 1992. Kinematics, topography, shortening, and extrusion in the India-Eurasia collision. *Tectonics* 11, 1085–1098.
- Macfarlane, A.M., 1993. Chronology of tectonic events in the crystalline core of the Himalaya, Langtang National Park, Central Nepal. *Tectonics* 12, 1004–1025.
- Macfarlane, A.M., 1995. An evaluation of the inverted metamorphic gradient at Langtang National Park, central Nepal Himalaya. *Journal of Metamorphic Geology* 13, 595–612.
- Makovsky, Y., Klemperer, S.L., 1999. Measuring the seismic properties of Tibetan bright spots: Evidence for free aqueous fluids in the Tibetan middle crust. *Journal of Geophysical Research* 104, 10,795–10,825.
- Metcalfe, R.P., 1993. Pressure, temperature, and time constraints on metamorphism across the Main Central Thrust zone and High Himalayan Slab in the Garwhal Himalaya. In: Searle, M.P., Treolar, P.J. (Eds.), *Himalayan Tectonics*, Geological Society of London Special Publication, 74, 485–509.
- Montel, J.-M., 1993. A model for monazite/melt equilibrium and application to the generation of granitic magmas. *Chemical Geology* 119, 127–146.
- Molnar, P., England, P., 1990. Temperatures, heat flux, and frictional stress near major thrust faults. *Journal of Geophysical Research* 95, 4833–4856.
- Molnar, P., Wang-Ping, C., Padovani, E., 1983. Calculated temperatures in overthrust terrains and possible combinations of heat sources responsible for the Tertiary granites in the Greater Himalaya. *Journal of Geophysical Research* 88, 6415–6429.
- Murphy, M.A., Harrison, T.M., 1999. The relationship between leucogranites and the South Tibetan detachment system, Rongbuk Valley, southern Tibet. *Geology* 27, 831–834.
- Nelson, K.D., et al., 1996. Partially molten middle crust beneath Southern Tibet: Synthesis of Project INDEPTH results. *Science* 274, 1684–1696.

- Nelson, K.D., Alsdorf, D., Unsworth, M., Zhao, W., Project, I.N.D.E.P.T.H. Team, 1999. Widespread melt in the Tibetan crust? In: 14th Himalaya-Karakorum-Tibet Workshop, Abstract volume, Kloster Ettal, Germany, pp. 108–109.
- Owens, T.J., Zandt, G., 1997. Implications of crustal property variations for models of Tibetan plateau evolution. *Nature* 387, 37–43.
- Pan, Y., Kidd, W.S.F., 1992. Nyainqentanghla shear zone: A Late Miocene extensional detachment in the southern Tibetan plateau. *Geology* 20, 775–778.
- Parrish, R.R., Hodges, K.V., 1996. Isotopic constraints on the age and provenance of the Lesser and Greater Himalayan sequences, Nepalese Himalaya. *Geological Society of America Bulletin* 108, 904–911.
- Patiño Douce, A., Harris, N., 1998. Experimental constraints on Himalayan anatexis. *Journal of Petrology* 39, 689–710.
- Patzelt, A., Li, H., Wang, J., Appel, E., 1996. Paleomagnetism of Cretaceous to Tertiary sediments from southern Tibet: evidence for the extent of the northern margin of India prior to the collision with Eurasia. *Tectonophysics* 259, 259–284.
- Pêcher, A., 1989. Metamorphism in the central Himalaya. *Journal of Metamorphic Petrology* 7, 31–41.
- Pinet, C., Jaupart, C., 1987. A thermal model for the distribution in space and time of the Himalayan granites. *Earth and Planetary Science Letters* 84, 87–99.
- Pognante, U., Benna, P., 1993. Metamorphic zonation, migmatization and leucogranites along the Everest transect of Eastern Nepal and Tibet: Record of an exhumation history. In: Searle, M.P., Treolar, P.J. (Eds.), *Himalayan Tectonics*, Geological Society of London Special Publication, 74, 323–340.
- Quidelleur, X., Grove, M., Lovera, O.M., Harrison, T.M., Yin, A., Ryerson, F.J., 1997. The thermal evolution and slip history of the Renbu Zedong Thrust, southeastern Tibet. *Journal of Geophysical Research* 102, 2659–2679.
- Ratschbacher, L., Frisch, W., Lui, G., Chen, C., 1994. Distributed deformation in southern and western Tibet during and after the India-Asia collision. *Journal of Geophysical Research* 99, 19,817–19,945.
- Rao, R.U.M., Rao, G.V., Narain, H., 1976. Radioactive heat generation and heat flow in the Indian Shield. *Earth and Planetary Science Letters* 30, 57–64.
- Rowley, D.B., 1996. Age of collision between India and Asia: A review of the stratigraphic data. *Earth and Planetary Science Letters* 145, 1–13.
- Royden, L.H., 1993. The steady state thermal structure of eroding orogenic belts and accretionary prisms. *Journal of Geophysical Research* 98, 4487–4507.
- Ruppel, C., McNamara, D.E., 1997. Seismic and rheological constraints on the thermal state of Tibetan Plateau upper mantle: Implications for melt production, mantle delamination, and large-scale tectonics. *EOS* 78, F650.
- Ruppel, C., Hodges, K.V., 1994. Pressure-temperature-time paths from two-dimensional thermal models: Prograde, retrograde and inverted metamorphism. *Tectonics* 13, 17–44.
- Rushmer, T., 1996. Melt segregation in the lower crust: How have experiments helped us? . *Transactions of the Royal Society of Edinburgh: Earth Science* 87, 73–83.
- Rutter, E.H., 1997. The influence of deformation on the extraction of crustal melts: a consideration of the role of melt assisted granular flow. In: Holmes, M.B. (Ed.), *Deformation Enhanced Fluid Transport in the Earth's Crust and Mantle*. Chapman & Hall, London, pp. 82–110.
- Schärer, U., 1984. The effect of initial ²³⁰Th disequilibrium on young U-Pb ages: The Makalu case. *Earth and Planetary Science Letters* 67, 191–204.
- Schärer, U., Xu, R.H., Allegre, C.J., 1986. U-(Th)-Pb systematics and ages of Himalayan leucogranites, South Tibet. *Earth and Planetary Science Letters* 77, 35–48.
- Schelling, D., 1992. The tectonostratigraphy and structure of the eastern Nepal Himalaya. *Tectonics* 11, 925–943.
- Schelling, D., Arita, K., 1991. Thrust tectonics, crustal shortening, and the structure of the far-eastern Nepal, Himalaya. *Tectonics* 10, 851–862.
- Searle, M.P., Rex, D.C., 1989. Thermal model for the Zaskar Himalaya. *Journal of Metamorphic Geology* 7, 127–134.
- Searle, M.P., Parrish, R.R., Hodges, K.V., Hurford, A., Ayres, M.W., Whitehouse, M.J., 1997. Shisha Pangma leucogranite, south Tibetan Himalaya: Field relations, geochemistry, age, origin, and emplacement. *Journal of Geology* 105, 295–317.
- Srivastava, P., Mitra, G., 1994. Thrust geometries and deep structure of the outer and lesser Himalaya, Kumaon and Garwal (India): Implications for evolution of the Himalayan fold-and-thrust belt. *Tectonics* 13, 89–109.
- Stüwe, K., Sandiford, M., 1994. Contribution of deviatoric stress to metamorphic P-T paths: An example appropriate to low-P, high-T metamorphism. *Journal of Metamorphic Geology* 12, 445–454.
- Swapp, S.M., Hollister, L.S., 1991. Inverted metamorphism within the Tibetan Slab of Bhutan — Evidence for a tectonically transported heat source. *Canadian Mineralogist* 29, 1019–1041.
- Thompson, A.B., 1982. Dehydration melting of pelitic rocks and the generation of H₂O-undersaturated granitic liquids. *American Journal of Science* 282, 1567–1595.
- Vance, D., Harris, N., 1999. The timing of prograde metamorphism in the Zaskar Himalaya. *Geology* 27, 395–398.
- Vance, D., Ayres, M., Kelley, S., Harris, N., 1998. The thermal response of a metamorphic belt to extension: constraints from laser Ar data on metamorphic micas. *Earth and Planetary Science Letters* 162, 153–164.
- Zhao, W., Nelson, K.D., Project, I.N.D.E.P.T.H., 1993. Deep seismic reflection evidence for continental underthrusting beneath southern Tibet. *Nature* 366, 557–559.